Materials Chemistry and Physics 291 (2022) 126560

Contents lists available at ScienceDirect

Materials Chemistry and Physics

journal homepage: www.elsevier.com/locate/matchemphys

Novel 5-(2-phenylbenzo[b]thiophen-3-yl)furan-2-carbaldehyde based ovarian cancer carbohydrate antigen 125 electrochemical sensor

Omer Faruk Er [a], Hilal Kivrak [b,c,d,*], Omruye Ozok [e], Arif Kivrak [e,**]

[a] Department of Chemical Engineering, Faculty of Engineering, Van Yuzuncu Yil University, Van, 65000, Turkey
[b] Department of Chemical Engineering, Faculty of Engineering and Architectural Sciences, Eskisehir Osmangazi University, Eskisehir, 26040, Turkey
[c] Translational Medicine Research and Clinical Center, Eskisehir Osmangazi University, 26040, Eskisehir, Turkey
[d] Kyrgyz-Turk Manas University, Faculty of Engineering, Department of Chemical Engineering, Bishkek, Kyrgyzstan, Turkey
[e] Department of Chemistry, Faculty of Sciences and Arts, Eskisehir Osmangazi University, Eskisehir, 26040, Turkey

HIGHLIGHTS

- 5-(2-phenylbenzo[b]thiophen-3-yl) furan-2-carbaldehyde (PTFC) is employed as antibody to detect CA125 antigen.
- Electrochemical results reveal that PTFC is a promising antibody for CA 125 antigen.
- Sensor has fairly wide linear range as 0.01–100 ng mL^{-1} and 100–1000 ng mL^{-1}

GRAPHICAL ABSTRACT

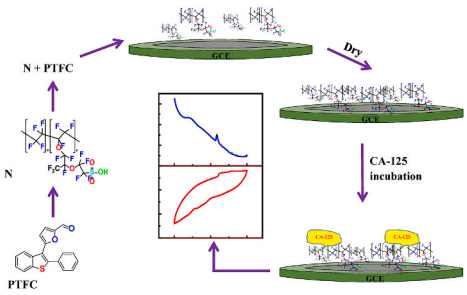

ARTICLE INFO

Keywords:
Benzothiophene
Electrochemical
Ovarian cancer
CA125
Sensor

ABSTRACT

Herein, an electrochemical sensor based 5-(2-phenylbenzo[b]thiophen-3-yl)furan-2-carbaldehyde (PTFC) was developed for the detection of cancer antigen 125 (CA125). Measurements were obtained via cyclic voltammetry (CV), electrochemical impedance spectroscopy (EIS), and differential pulse voltammetry (DPV), and square wave voltammetry (SWV) techniques to investigate features of the electrochemical sensor such as concentration effect of CA125, incubation time, scan rate, limit of quantification (LOQ), limit of detection (LOD), and interference effect of structures found in serum. The sensor was found to have a fairly wide linear range as 0.01–100 ng mL^{-1} and 100–1000 ng mL^{-1}. LOQ and LOD values were determined as 0.024015 ng mL^{-1} and 0.008005 ng mL^{-1} (S/N = 3), respectively. These results showed that the PTFC-based electrode could be a promising electrode for the detection of CA125.

* Corresponding author. Department of Chemical Engineering, Faculty of Engineering and Architectural Sciences, Eskisehir Osmangazi University, Eskisehir, 26040, Turkey.
** Corresponding author.
E-mail addresses: hilalkivrak@gmail.com, hilaldemir.kivrak@ogu.edu.tr (H. Kivrak), arif.kivrak@ogu.edu.tr (A. Kivrak).

https://doi.org/10.1016/j.matchemphys.2022.126560
Received 2 March 2022; Received in revised form 18 July 2022; Accepted 19 July 2022
Available online 10 August 2022

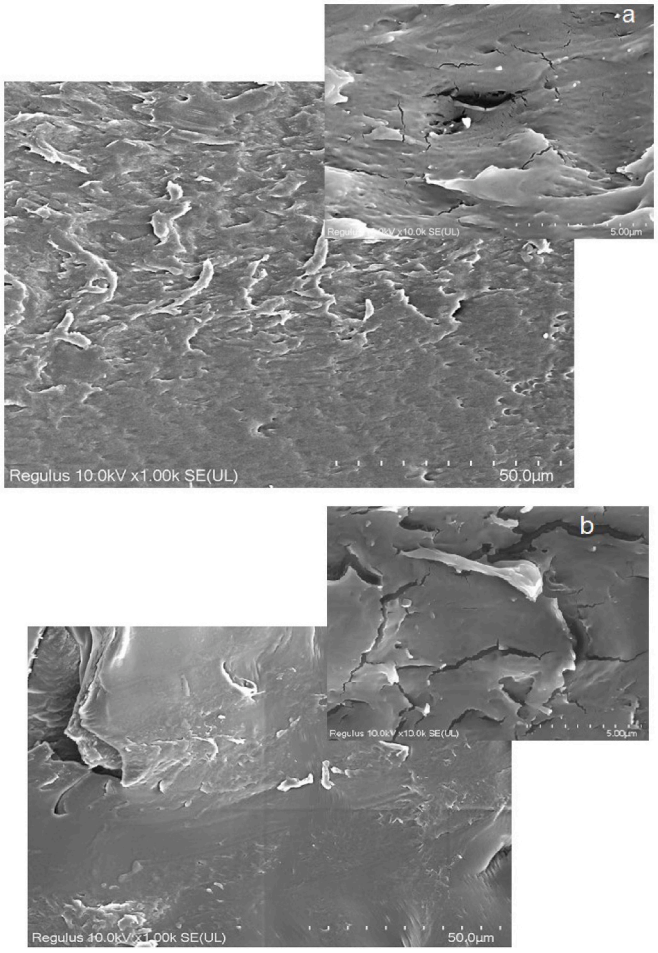

Fig. 1. SEM images of (a) PTFC and (b) Nafion modified PTFC at 500 μm, insert shows 5 μm resolution.

1. Introduction

Cancer is a disease caused by the transformation of cells that become abnormal and proliferate excessively. These deregulated cells sometimes end up forming a mass called a malignant tumor. Cancer cells tend to invade nearby tissues and break away from the original tumor. They then migrate through the blood vessels and lymphatic vessels to form another tumor. Ovarian cancer (OC) is one of the deadliest diseases see in women worldwide, and one of the cancer type that is difficult to diagnose early due to the absence of symptoms in the early stages and the lack of screening strategies on the market. Ovarian cancer usually occurs as a complex mass in the pelvis of the ovaries. It has different behaviors at molecular, cellular, and clinical levels. In advanced stages, metastases can rub on to the lung and liver via blood vessels or to nodes in the renal hilum via lymphatics [1–4]. If early detection systems can be developed, OC can be treated with platinum-based chemotherapy or surgery [5–7].

Tumor markers are molecules that may be produced as a response by the body either in cancer presence or in conditions such as inflammation. These biomarkers can also be released by tumors of cancers. These are very important proteins that can be an indicator of disease stages according to levels inside serum. Developing cost-effective, reliable, monitoring strategies, and strong detections for cancer is crucial, especially now because of the high death rates, high recurrence rates, and prevalence of the disease. They are used in diagnosis, follow-up detection of recurrence, and evaluation of cancer stages [8–12]. Tumor markers can be traced by measuring them in tissue or serum for early diagnosis of cancer [13–17]. Cancer antigen 125 (CA125) is the only marker used among tumor markers to trace ovarian cancer. CA125 is a glycoprotein greater than 200 kDa, and the normal value of CA125 in human blood is between 0 and 35 U mL^{-1} [18–20]. CA125 antigen could found in most serosal fluids due to secreted from serosal epithelial cells. In the presence of ovarian cancer, CA125 level increases in the blood, while the level of CA125 in the blood may increase also in diseases such as heart failure obstruction, abdominal surgery, peritoneal infection, and liver cirrhosis [21–26]. The organic based sensor elements may be functionalized with biospecific probe organic molecules. They increase the biospecificity of target protein markers detection. Benzothiophene derivatives including aldehyde functional groups allow to conduct the target proteins in sample. Hence, organic based biosensors improved the following advantages: (i) highly sensitive of target proteins, (ii) rapid analysis of target proteins, and (iii) lower cost for detection procedure [27,28].

Recently, various methods such as fluorescence [29–31], liquid phase immunoassay [32], colorimetric immunoassay [18,33], optical biosensors [34], and electrochemical sensor [35–37] have been employed to accurately and more sensitively trace the level of CA125 in serum. Due to the fact that electrochemical sensors have superior features such as appropriate cost, simple design, specificity, simple use, miniaturization, and easy transport, studies on electrochemical sensors have been increased in recent years [38–41]. To enhance sensitivities and accuracy of the electrochemical sensors to follow-up CA125 level in serum medium, micro-sensor chips were used and studied on the materials as Au-VBG/BDD electrode [42–44], MPA/AuNPs@SiO_2/QD/-mAb [45], Ag NPs-GQDs [46], g-C_3N_4 [47], and Cys-AuNPs/ERGO probes [48]. In addition, Ravalli et al. developed a graphite electrode-based CA125 immunosensor modified with gold nanoparticles. They reported that this sensor showed a linear variation in CA125 antigen concentrations among 0–100 U mL^{-1}, and the detection limit was also estimated as 6.7 U mL^{-1} [49]. In another study, Chen et al. indicated that $Co(bpy)_3^{3+}$ structure was initially connected on MWCNTs-N film and then modified with nano-Au and anti-CA125 structures on $Co(bpy)_3^{3+}$/MWCNTs-N film, respectively. It was reported that the developed sensor had high sensitivity consisting of a detection limit of 0.36 U mL^{-1} and had two linear ranges as 1–30 U mL^{-1} and 30–150 U mL^{-1} [50]. In the same way, Tang et al. reported that thionine−horseradish peroxidase (TH-HRP) composite was prepared for the detection of CA125 in serum and anti-CA125 was attached to its surface. As a result, immunosensor had a detection limit of 0.1 U mL^{-1} and a wide working range among 0.1–450 U mL^{-1} [51]. Torati et al. reported that it was developed an immunosensor based on gold nanostructures and that sensor exhibited a linear range of 10–100 U mL^{-1} and a low detection limit of 5.5 U mL^{-1} [52].

In this study, we developed an organic electrochemical sensor that had a high selectivity to detect CA125 in serum medium by using a benzothiophene core. Initially, 5-(2-phenylbenzo[b]thiophen-3-yl) furan-2-carbaldehyde (PTFC) structure was synthesized, and PTFC structure was characterized by ^{13}C NMR and ^{1}H NMR, LC-MS/MS, SEM, and FT-IR. Finally, measurements were performed CV, EIS, DPV, and SWV techniques over electrodes prepared with PTFC at room temperature.

2. Materials and methods

At present, PTFC was synthesized, characterized, and employed as CA125 electrochemical sensor by modifying on GCE electrode. The necessary materials and equipments were given in the support file S1; synthesis method and characterization details were presented in S.2, **the Surface properties of PTFC materials were characterized by scanning electron microscopy.** Finally, measurements were performed CV, EIS, DPV, and SWV techniques over electrodes prepared with PTFC at room temperature. Fabrication of the electrochemical sensor was given S3. The details of electrochemical measurements were explained at S.4.

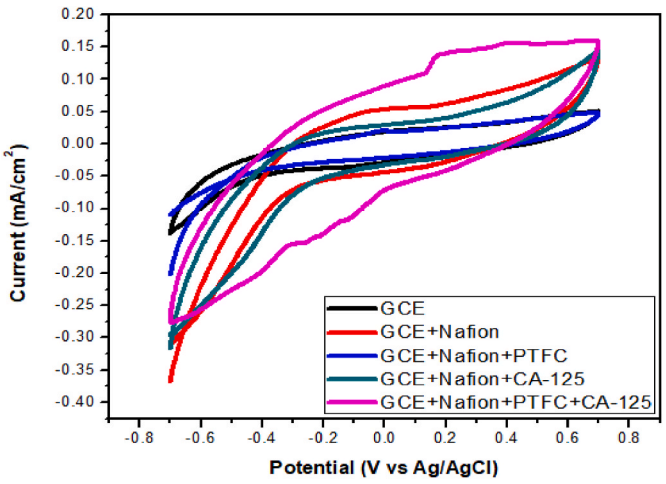

Fig. 2. CV results for GCE, GCE + N, GCE + N + PTFC, GCE + N + CA125, and GCE + N + PTFC + CA125 electrodes at 1000 ng mL^{-1} CA125 in pH: 7.4 PBS+5 mM $Fe(CN)_6^{3/4-}$ (scan rate = 50 mV s^{-1} and room temperature).

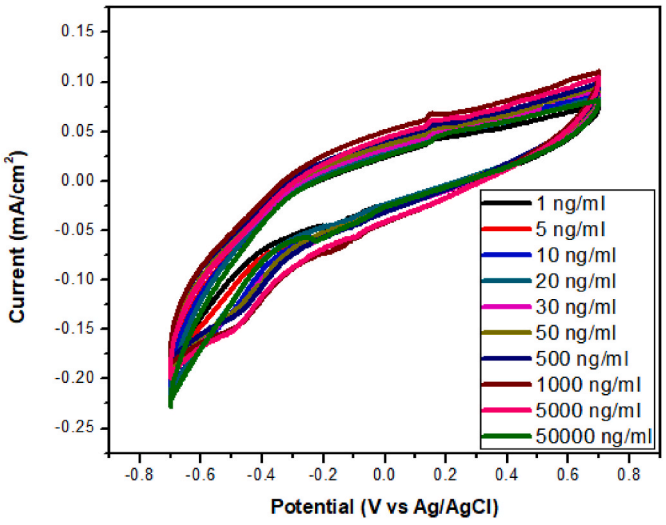

Fig. 3. CV results that taken at room temperature in pH: 7.4 PBS+5 mM Fe $(CN)_6^{3-/4-}$ solution for GCE + N + PTFC + CA125 electrodes prepared at 30 min incubation time with varying values concentrations among 1–50000 ng mL^{-1} CA125.

3. Results and discussion

Synthesis procedure and ^{13}C NMR and ^{1}H NMR results of PTFC were presented in S2. ^{13}C NMR and ^{1}H NMR results revealed that these materials were successfully prepared. Furthermore, the surface properties of PTFC materials were characterized by scanning electron microscopy. The Nafion modified electrode surface SEM images were also taken in order to understand the effect of the Nafion modification on the PTFC. SEM images were given in Fig. 1. From the images it is clear that there is no considerable difference in the surface structure of organic materials.

An electrochemical sensor was developed with PTFC structure for detection CA125 antigen of the OC in serum medium. All measurements taken over this sensor were performed via CV, EIS, DPV, and SWV techniques. Firstly, measurements were received by CV technique over GCE, GCE + Nafion (N), GCE + N + CA125, GCE + N + PTFC, and GCE + N + PTFC + CA125 electrodes. Results of these measurements were given in Fig. 2. The GCE + N + CA125 and the GCE + N + PTFC + CA125 electrodes were prepared at room temperature by incubating of 1000 ng mL^{-1} CA125 amount for 30 min. The current values of GCE and GCE + N + PTFC electrodes with GCE + N and GCE + N + CA125 electrodes were close to each other (Fig. 2). In addition, forward and backward peaks were not observed in peaks of these electrodes. GCE + N + PTFC + CA125 electrode revealed the best performance with values forward peaks 0.146 mA cm^{-2} (146.0 μA cm^{-2}) at 0.22 V and backward

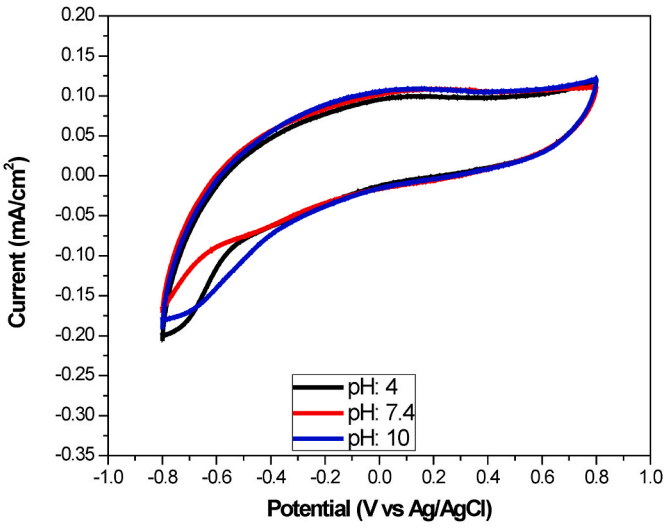

Fig. 5. GCE + N + PTFC + CA125 electrode prepared with 1000 ng mL^{-1} at 30 min incubation time at between 50 mV s^{-1} scan rates at varying pHs PBS+5 mM $Fe(CN)_6^{3-/4-}$ at room temperature.

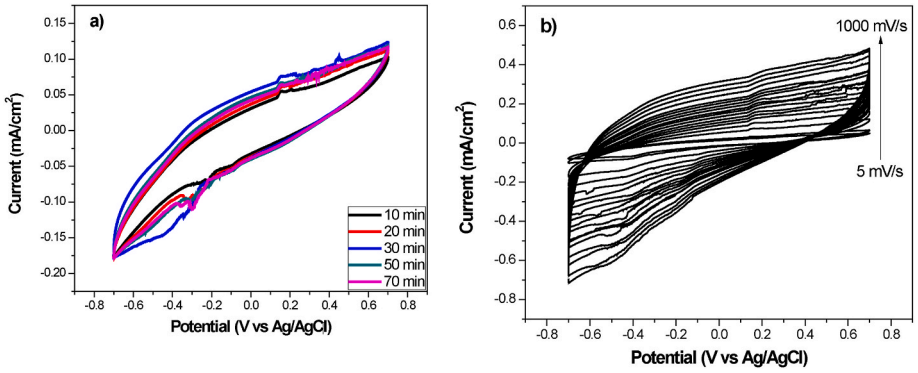

Fig. 4. CV results for **a)** GCE + N + PTFC + CA125 electrode prepared with 1000 ng/mL CA125 at varying incubation times of 10–70 min (scan rate: 50 mV s^{-1}); **b)** [illegible] $(CN)_6^{3-/4-}$ at room temperature.

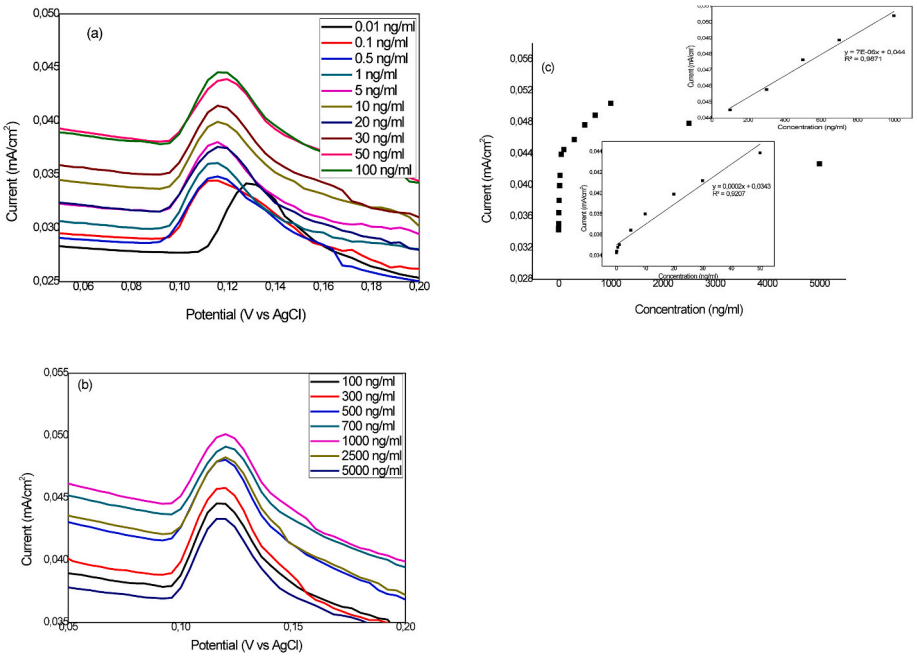

Fig. 6. DPV results received at room temperature in pH: 7.4 PBS+5 mM $Fe(CN)_6^{3-/4-}$ solution on GCE + N + PTFC + CA125 electrodes produced with varying rates between **a)** 0.01–100 ng mL^{-1} CA125, **b)** 100–5000 ng mL^{-1} CA125 for 30 min incubation time, and c) maximum current against concentration values.

Table 1
Properties of electrochemical sensors used to detect CA125 compiled from literature.

Tumor marker	sensor	LOD or LOQ	Linear range	Ref.
CA125	Anti-CA125/GHM/PTH/GCE	1.3 U/mL	4.5–36.5 U/mL	[53]
CA125	CA125/CANs/CA-GCE	1.73 U/mL	0–30 U/mL	[54]
CA125	MWCNT-ZnO	0.00113 U/mL	0.001 U/mL-1 kU/mL	[55]
CA125	AuNP-PB-PtNP-PANI hydrogel	4.4 mU/mL	0.01–5000 U/mL	[56]
CA125	Au/PDDA/PTCA/CNTs/redox-probe@D-Ab	3.3 pg/mL	0.012–12 ng/mL	[57]
CA125	Au–Thi-CPEs	1.8 U/mL	10–30 U/mL	[58]
CA125	CNF-based	1.8 U/mL	2–75 U/mL	[59]
CA125	CNTs-based	0.9 U/mL	3–200 U/mL	[60]
CA125	**GCE + N + PTFC DPV**	**0.008005 ng mL^{-1} (LOD)**	**0.01–50 ng/mL 100–1000 ng/mL**	**In this study**
CA125	**GCE + N + PTFC SWV**	**0.024015 ng mL^{-1} (LOQ)**	**1–50 ng/mL 100–700 ng/mL**	**In this study**

peak 0.157 mA cm^{-2} (157.0 μA cm^{-2}) at −0.26 V (Fig. 2). This phenomenon could be attributed to the fact that CA125 binds to the PTFC structure in the sensor and an electrochemical event occurs between the two structures.

To research, the effect of CA125 concentration on the electrochemical sensor was prepared electrodes varying among 1–50000 ng mL^{-1} CA125 amounts. These electrodes were obtained by incubating CA125 for 30 min over GCE + N + PTFC electrodes at room temperature. Measurements were taken in pH: 7.4 PBS+5 mM $Fe(CN)_6^{3-/4-}$ solution via CV and the results are shown in Fig. 3 (scan rate = 50 mV s^{-1}). A gradual increase among 1 ng mL^{-1} (0.042 mA cm^{-2} at 0.15 V)-1000 ng mL^{-1} (0.071 mA cm^{-2} at 0.15 V) and a gradual increase among 1000 ng mL^{-1}-50,000 ng mL^{-1} (0.045 mA cm^{-2} at 0.17 V) were observed in the results. 1000 ng mL^{-1} was determined the best concentration value of CA125 for the electrochemical sensor.

To investigate the effect of scan rate over electrooxidation process among PTFC structure with CA125 and to determine the best incubation time of the electrochemical sensor were taken measurements via CV in pH: 7.4 PBS+5 mM $Fe(CN)_6^{3-/4-}$ solution. These results were shown in Fig. 4. Initially, measurements to research incubation time were performed over GCE + N + PTFC + CA125 electrodes prepare by incubating 1000 ng mL^{-1} CA125 varying times among 10–70 min (Fig. 4a). As a result, optimum electrode time preparation was found 30 min. Afterward, it was obtained measurements at different scan rates among 5–1000 mV s^{-1} over GCE + N + PTFC + CA125 electrodes prepared by incubating 1000 ng mL^{-1} CA125 for 30 min (Fig. 4b). In the measurements, it was observed that the current density increased as the scan rate increased from 5 to 1000 mV/s, which indicated that a diffusion-controlled reaction took place in the electrochemical sensor.

The effect of pH was performed at three different pH values on GCE + N + PTFC + CA125 electrode prepared with 1000 ng/mL CA125 at 30 min incubation time. CV measurements were given in Fig. 5. Results revealed that pH did not have significant effect on electrooxidation activity:

DPV measurements were taken on the electrodes in 0.1 M PBS at varying concentrations (0.01–5000 ng/mL CA 125 antigen), shown in Fig. 6a–b. DPV results revealed while concentration of CA125 antigen increases from 0.01 ng/mL to 1000 ng/mL, the DPV current density increase. When 1000 ng/mL is reached, DPV current densities starts to decrease slightly. The calibration plot of the DPV peak current densities versus concentration of CA125 antigen is also illustrated in Fig. 6c. One can note that the DPV current densities versus CA125 antigen concentration plot exhibited a linear relationship within the range of 0.01–50 ng/mL and 100–1000 ng/mL, revealing that there are two linear regions. These linear range vales are higher than reported in literature given in Table 1.

On the other hand, by using SWV technique, we obtain the linear range value from SWV. Similar to DPV measurements, SWV measurements were performed on the electrodes in 0.1 M PBS at varying concentrations (0.01–5000 ng/mL CA 125 antigen). The SWV results were presented in Fig. 7. The SWV results obtained at 0.01–5000 ng/mL CA

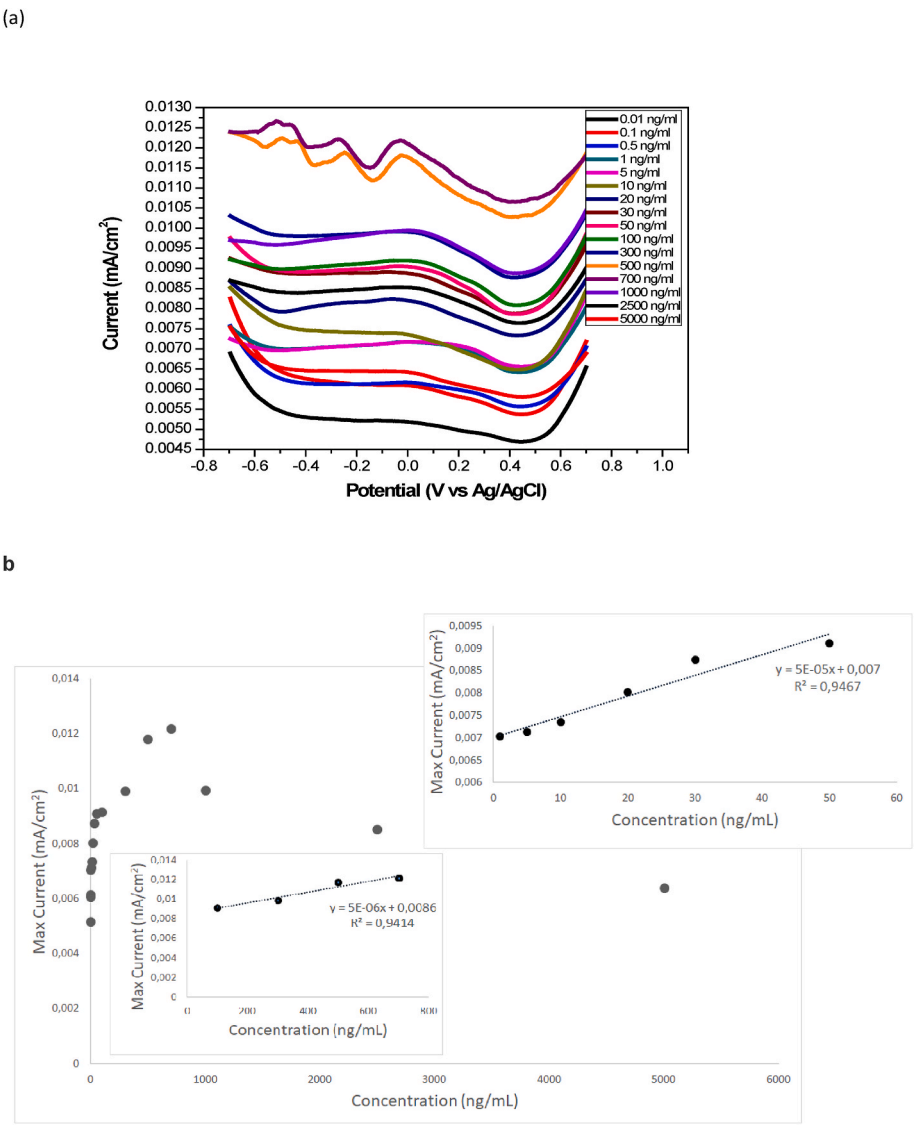

Fig. 7. SWV results received at room temperature in pH: 7.4 PBS+5 mM $Fe(CN)_6^{3-/4-}$ solution on GCE + N + PTFC + CA125 electrodes produced with varying rates between **a)** 0.01–5000 ng mL^{-1} CA125 for 30 min incubation time, and b) maximum current against concentration values.

125 antigen was presented Fig. 7a. It clear that when CA125 antigen concentration increased, the SWV current density increased. In Fig. 7b, SWV current densities were plotted and given and insets in Fig. 7-b shows the linear regions. Two linear region was obtained fro, SWV. These linear regions are 0.01–50 ng/mL and 100–700 ng/mL, respectively. These linear regions obtained form SWV are in agreements ones from the obtained DPV.

Limit of blank (LOB), lowest detection limit (LOD), and limit of quantification (LOQ), which is known as the lowest concentration value, values at acceptable sensitivity for the designed electrochemical sensor were calculated with GCE + N + PTFC electrode and GCE + N + PTFC + CA125 electrodes. Limit of Blank (LoB), Limit of Detection (LoD), and Limit of Quantitation (LoQ) are terms used to describe the smallest concentration of a measurand that can be reliably measured by an analytical procedure. LoB is the highest apparent analyte concentration expected to be found when replicates of a blank sample containing no analyte are tested. LoD is the lowest analyte concentration likely to be reliably distinguished from the LoB and at which detection is feasible. LoD is determined by utilising both the measured LoB and test replicates of a sample known to contain a low concentration of analyte. To define the LOB value, 10 blank measurements were taken on the GCE + N + PTFC electrode without CA125, and then the standard deviation was determined. DPV, 10 blank measurements, and concentration values vs. maximum currents were given in Fig. 8. LOQ, LOB, and LOD values were calculated by using following equations:

$$\text{LoB} = \text{meanblank} + 1.645(\text{SD}_{\text{blank}}) \quad 2.1$$

$$\text{LoD} = \text{LoB} + 1.645(\text{SD}_{\text{low concentration sample}}) \quad 2.2$$

$$\text{LoQ} = 3\ \text{LoQ}\ (\text{S/N} = 3) \quad 2.3$$

LOQ, LOB, and LOD values were determined as 0.024015 ng mL^{-1}, 0.007516 ng mL^{-1}, and 0.008005 ng mL^{-1} (S/N = 3), respectively. It can be clearly seen that the LOD value found for this sensor is lower than the sensors noticed in the literature.

EIS is a technique used widely by characterizing electrochemical systems. This technique is utilized widely in areas like medicine, electrochemistry, and material science [37]. The Nyquist plots are obtained from EIS data. These plots are being in a semicircular providing informant about load transfer resistance in systems [37,40,61–63]. In addition, EIS data could be correlated to microstructural properties, rates of reaction and diffusion [62]. In this study, EIS measurements were performed with GCE + N + PTFC + CA125 electrodes prepared by incubating 1000 ng mL^{-1} (30 min) at varying potentials between −0.6 V and

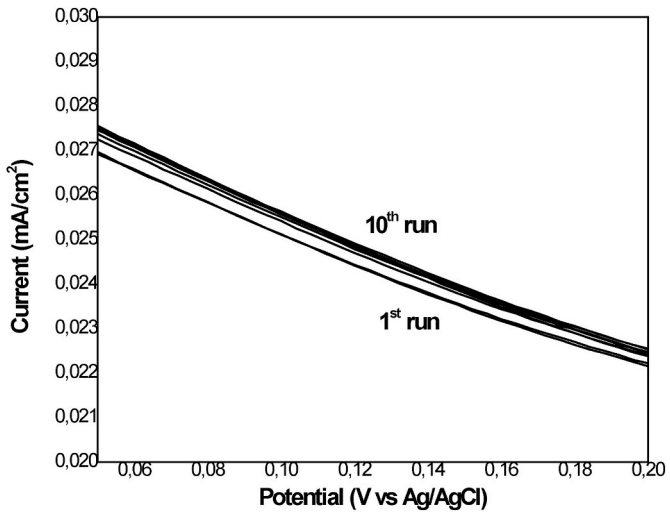

Fig. 8. DPV results received at room temperature in pH: 7.4 PBS+5 mM Fe $(CN)_6^{3-/4-}$ solution on GCE + N + PTFC electrodes prepared without CA125 antigen (10 blank electrodes).

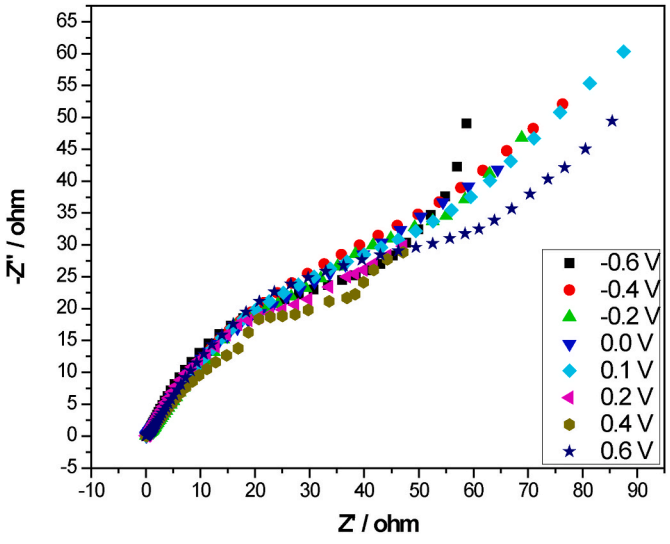

Fig. 9. Nyquist Plots obtained that EIS measurements received at room temperature in pH: 7.4 PBS+5 mM $Fe(CN)_6^{3-/4-}$ solution at varying potentials among −0.6 and 0.6 V on GCE + N + PTFC + CA125 electrodes prepared with 1000 ng mL^{-1} CA125 for 30 min incubation time.

Table 2
Stability and repeatability results.

Measurement	Cycle number	Max DPV current	Relative Current (%)	RSD (%)
stability	1st	0.0490	100	0
	20th	0.0486	99.2	0.8
	50th	0.0475	96.2	3.8
	75th	0.0468	95.5	4.5
	100th	0.0457	93.26	6.7
repeatability	Electrode number	Max DPV current	RSD (%)	
	1st	0.0490	0	
	2nd	0.0483	1.43	
	5th	0.0453	7.55	
	10th	0.0519	−5.91	

0.6 V in pH: 7.4 PBS+5 mM $Fe(CN)_6^{3-/4-}$ solution at room temperature. These results were shown in Fig. 9. Herein, it can be explained that a low charge transfer resistance when the semicircles are small in diameter, and a large charge transfer resistance when the semicircles are large in diameter throughout electrooxidation among PTFC structure and CA125 in the electrochemical sensor. It watched that close to each other semicircle diameters of all electrodes in measurements performed among −0.6 V–0.6 V, and the lowest load transfer resistance was acquired over 0.4 potential. These results are suitable with DPV and CV results.

According to CV, DPV and EIS results, the following electrooxidation mechanism was proposed;

Step 1: PTFC + CA125 antigen [PTFC … CA125 antigen] 2.4
Step 2: [PTFC … CA125 antigen] + OH^- → PTFC + H_2O + intermediates + e^- 2.5

After DPV, EIS, and CV results over electrooxidation sensor, it was performed interference measurements for structures that find in blood samples like ascorbic acid, uric acid, glucose, and dopamine, which can affect the electrooxidation operation among PTFC and CA125. In addition, these measurements are determined the sensitivity of the electrochemical sensor. EIS measurements 0.4 potential and CV measurements were received over GCE + N + PTFC electrodes and GCE + N + PTFC + CA125 electrodes that prepared with 1000 ng mL^{-1} CA125 (30 min incubation time) in 0.1 mM ascorbic acid + pH: 7.4 PBS, 2.5 mM uric acid + pH: 7.4 PBS, 0.1 mM dopamine + pH: 7.4 PBS, and 4.7 mM D-glucose + pH: 7.4 PBS solutions. It was given CV results in Fig. S1 and EIS results in Fig. S3. The forward peaks that be electrooxidation peak at 0.2 potential were not observed in all CV measurements performed over GCE + N + PTFC electrodes. Moreover, glucose, ascorbic acid, and dopamine showed similarly and lower interference effects, while uric acid showed a higher interference effect from these (Fig. S1). However, it can be said that not affect electrooxidation operation among CA125 and PTFC of uric acid (Fig. S1a). The Nyquist plots obtained from EIS measurements taken over electrodes without CA125 were observed similar results. The load transfer resistance (Rct) in measurements performed without CA125 was the highest, in the presence of CA125 was found that be also low (Fig. S2). All these results prove that not affect electrooxidation operation that is among PTFC and CA125 in the electrochemical sensor of structures such as glucose, ascorbic acid, uric acid, and dopamine that find in blood samples. Furthermore, these results show also that the PTFC structure has a high sensitivity to CA125.

Finally, to investigate the effect of salts that find in blood samples on the electrochemical sensor was taken measurements in mediums of artificial and isotonic serum. These measurements were performed via CV and EIS (0.4 V) techniques over GCE + N + PTFC + CA125 electrodes prepared at room temperature with 1000 ng mL^{-1} CA125 (30 min incubation time). It is given results obtained in Fig. S3. As seen in Fig. S3a, it was found to exhibit a high interference-effect of artificial serum according to isotonic serum. However, it is clearly seen that not affect the electrooxidation process among PTFC and CA125 in the electrochemical sensor. EIS results at 0.4 potential of artificial and isotonic serum were exhibited also by each other very close load transfer resistances (Fig. S3b).

Stability studies were performed on PTFC by DPV. Taking 100 cycles on GCE + N + PTFC + CA125 electrodes prepared with 1000 ng mL^{-1} CA125 for 30 min incubation time. The maximum current values for 1st, 20th, 50th, 75th, 100th current values were given in Table 2. Results show that relative current values from 1st to 100th cycle decrease form 100% to 93.26%. Relative deviation values were given also. These values are below the 10%. This value could be acceptable for stability measurements. These values show that results are repeatable and electrode surface does not change after sensor measurements. To obtain repeatability results, 10 different GCE + N + PTFC + CA125 electrodes were prepared with 1000 ng mL^{-1} CA125 for 30 min incubation time

and repeatability measurements were done on these electrodes by DPV. Maximum DPV values were recorded for these 10 electrodes. For 1st, 2nd, 5th, 7th, 10th electrodes maximum DPV values were given in Table 2. For the repeatability measurements RSD values show that results are repeatable.

4. Conclusions

PTFC structure that is benzothiophene derivative was synthesized for determining CA125 antigen in serum medium with electrochemical methods like CV, EIS, and DPV. Important parameters affecting electrochemical sensor sensitivity like concentration value of CA125, incubation time, scan rate, interference effect were examined via these methods. It was observed two different linear areas for the electrochemical sensor prepared including the first linear area 0.01–50 ng mL^{-1} and the second linear area 100–1000 ng mL^{-1}. Moreover, LOQ and LOD values for the sensor were obtained as 0.024015 ng mL^{-1} and 0.008005 ng mL^{-1} (S/N = 3), respectively. One can be clearly seen that the sensor prepared with PTFC has a wide linear area and higher sensitivity than the linear range values reported in the literature. In addition, the LOD value was also lower than the LOD values reported in the literature. Artificial serum and interference results disclose that a promising electrode for the detection of CA125. According to all electrochemical results obtained, the PTFC structure can clearly see that a promising antibody due to its high sensitivity in detecting CA125 used in the diagnosis of OC and superior properties such as acceptable LOD and LOQ values.

CRediT authorship contribution statement

Omer Faruk Er: Visualization, Investigation, Writing – original draft, Data curation. **Hilal Kivrak:** Conceptualization, Methodology, Supervision, Writing – review & editing. **Omruye Ozok:** Visualization, Investigation. **Arif Kivrak:** Conceptualization, Methodology, Supervision, Writing – review & editing.

Declaration of competing interest

The authors declare that they have no known competing financial interests or personal relationships that could have appeared to influence the work reported in this paper.

Data availability

Data will be made available on request.

Acknowledgements

O. Faruk ER thank to the Council of Higher Education (YOK) for 100/2000 scholarship and the Scientific and Technological Research Council of Turkey (TUBITAK) for 2211-A scholarship.

Appendix A. Supplementary data

Supplementary data to this article can be found online at https://doi.org/10.1016/j.matchemphys.2022.126560.

References

[1] S.M. Majd, A. Salimi, Ultrasensitive flexible FET-type aptasensor for CA 125 cancer marker detection based on carboxylated multiwalled carbon nanotubes immobilized onto reduced graphene oxide film, Anal. Chim. Acta 1000 (2018) 273–282.
[2] R.C. Bast, B. Hennessy, G.B. Mills, The biology of ovarian cancer: new opportunities for translation, Nat. Rev. Cancer 9 (2009) 415–428.
[3] A.J. Cortez, P. Tudrej, K.A. Kujawa, K.M. Lisowska, Advances in ovarian cancer therapy, Cancer Chemother. Pharmacol. 81 (2018) 17–38.
[4] Z. Momenimovahed, A. Tiznobaik, S. Taheri, H. Salehiniya, Ovarian cancer in the world: epidemiology and risk factors, Int. J. Wom. Health 11 (2019) 287.
[5] B. Deb, A. Uddin, S. Chakraborty, miRNAs and ovarian cancer: an overview, J. Cell. Physiol. 233 (2018) 3846–3854.
[6] G.C. Jayson, E.C. Kohn, H.C. Kitchener, J.A. Ledermann, Ovarian cancer, Lancet 384 (2014) 1376–1388.
[7] U.A. Matulonis, A.K. Sood, L. Fallowfield, B.E. Howitt, J. Sehouli, B.Y. Karlan, Ovarian cancer, Nat. Rev. Dis. Prim. 2 (2016) 1–22.
[8] S.N. Han, A. Lotgerink, M.M. Gziri, K. Van Calsteren, M. Hanssens, F. Amant, Physiologic variations of serum tumor markers in gynecological malignancies during pregnancy: a systematic review, BMC Med. 10 (2012) 86.
[9] S. Rauf, G.K. Mishra, J. Azhar, R.K. Mishra, K.Y. Goud, M.A.H. Nawaz, J.L. Marty, A. Hayat, Carboxylic group riched graphene oxide based disposable electrochemical immunosensor for cancer biomarker detection, Anal. Biochem. 545 (2018) 13–19.
[10] B.V. Chikkaveeraiah, A.A. Bhirde, N.Y. Morgan, H.S. Eden, X. Chen, Electrochemical immunosensors for detection of cancer protein biomarkers, ACS Nano 6 (2012) 6546–6561.
[11] J.D. Wulfkuhle, L.A. Liotta, E.F. Petricoin, Proteomic applications for the early detection of cancer, Nat. Rev. Cancer 3 (2003) 267–275.
[12] V. Kulasingam, E.P. Diamandis, Strategies for discovering novel cancer biomarkers through utilization of emerging technologies, Nat. Clin. Pract. Oncol. 5 (2008) 588–599.
[13] J.F. Rusling, C.V. Kumar, J.S. Gutkind, V. Patel, Measurement of biomarker proteins for point-of-care early detection and monitoring of cancer, Analyst 135 (2010) 2496–2511.
[14] I.E. Tothill, Biosensors for cancer markers diagnosis, in: Seminars in Cell & Developmental Biology, Elsevier, 2009, pp. 55–62.
[15] Z. Xiao, D. Prieto, T.P. Conrads, T.D. Veenstra, H.J. Issaq, Proteomic patterns: their potential for disease diagnosis, Mol. Cell. Endocrinol. 230 (2005) 95–106.
[16] M.P. Ebert, M. Korc, P. Malfertheiner, C. Röcken, Advances, challenges, and limitations in serum-proteome-based cancer diagnosis, J. Proteome Res. 5 (2006) 19–25.
[17] E. Stevens, L. Liotta, E.C. Kohn, Proteomic analysis for early detection of ovarian cancer: a realistic approach? Int. J. Gynecol. Cancer 13 (2003) 133–139.
[18] O. Hosu, A. Ravalli, G.M.L. Piccolo, C. Cristea, R. Sandulescu, G. Marrazza, Smartphone-based immunosensor for CA125 detection, Talanta 166 (2017) 234–240.
[19] I. Diaconu, C. Cristea, V. Hârceagă, G. Marrazza, I. Berindan-Neagoe, R. Săndulescu, Electrochemical immunosensors in breast and ovarian cancer, Clin. Chim. Acta 425 (2013) 128–138.
[20] R. Lahoud, A. O'Shea, C. El-Mouhayyar, I. Atre, K. Eurboonyanun, M. Harisinghani, Tumour Markers and Their Utility in Imaging of Abdominal and Pelvic Malignancies, Clinical Radiology, 2020.
[21] K.A. Sikaris, CA125—a test with a change of heart, Heart, Lung Circ. 20 (2011) 634–640.
[22] M. Epiney, C. Bertossa, A. Weil, A. Campana, P. Bischof, CA125 production by the peritoneum: in-vitro and in-vivo studies, Hum. Reprod. 15 (2000) 1261–1265.
[23] M. Ulusoy, A. Ayer, H. Feyizoğlu, M.S. Alan, K. Keskin, Y. Gürkan, I. Cengiz, Z. Kuyubaşi, Tuberculous peritonitis and elevated serum CA 125 in a patient with chronic renal failure, Turk. J. Gastroenterol. 16 (2005) 117–118.
[24] M. Eerdekens, E. Nouwen, D. Pollet, T. Briers, M. De Broe, Placental alkaline phosphatase and cancer antigen 125 in sera of patients with benign and malignant diseases, Clin. Chem. 31 (1985) 687–690.
[25] C.A. Yedema, P. Kenemans, C.M. Thomas, L.F. Massuger, T. Wobbes, R. Verstraeten, J. Hilgers, G. van Kamp, CA 125 serum levels in the early post-operative period do not reflect tumour reduction obtained by cytoreductive surgery, Eur. J. Cancer 29 (1993) 966–971.
[26] R. Sessler, H. Konyar, G. Hasche, C.J. Olbricht, The haemodialysis patient with night sweats, ascites, and increased CA 125, Nephrol. Dial. Transplant. 16 (2001) 175–177.
[27] K.A. Malsagova, T.O. Pleshakova, R.A. Galiullin, A.F. Kozlov, I.D. Shumov, V. P. Popov, F.V. Tikhonenko, A.V. Glukhov, V.S. Ziborov, O.F. Petrov, V.E. Fortov, A. I. Archakov, Y.D. Ivanov, Highly sensitive detection of CA 125 protein with the use of an n-type nanowire biosensor, Biosensors 10 (2020).
[28] M.R. Awual, Novel conjugated hybrid material for efficient lead(II) capturing from contaminated wastewater, Mater. Sci. Eng. C Mater. Biol. Appl. 101 (2019) 686–695.
[29] X. Xu, J. Ji, P. Chen, J. Wu, Y. Jin, L. Zhang, S. Du, Salt-induced gold nanoparticles aggregation lights up fluorescence of DNA-silver nanoclusters to monitor dual cancer markers carcinoembryonic antigen and carbohydrate antigen 125, Anal. Chim. Acta 1125 (2020) 41–49.
[30] D. Sok, L.-J.A. Clarizia, L.R. Farris, M.J. McDonald, Novel fluoroimmunoassay for ovarian cancer biomarker CA-125, Anal. Bioanal. Chem. 393 (2009) 1521–1523.
[31] M.R. Awual, Novel nanocomposite materials for efficient and selective mercury ions capturing from wastewater, Chem. Eng. J. 307 (2017) 456–465.
[32] M. Terenghi, L. Elviri, M. Careri, A. Mangia, R. Lobinski, Multiplexed determination of protein biomarkers using metal-tagged antibodies and size exclusion chromatography– inductively coupled plasma mass spectrometry, Anal. Chem. 81 (2009) 9440–9448.
[33] W. Hong, S. Lee, Y. Cho, Dual-responsive immunosensor that combines colorimetric recognition and electrochemical response for ultrasensitive detection of cancer biomarkers, Biosens. Bioelectron. 86 (2016) 920–926.
[34] I. Al-Ogaidi, H. Gou, Z.P. Aguilar, S. Guo, A.K. Melconian, A.K.A. Al-Kazaz, F. Meng, N. Wu, Detection of the ovarian cancer biomarker CA-125 using

chemiluminescence resonance energy transfer to graphene quantum dots, Chem. Commun. 50 (2014) 1344–1346.
[35] E.B. Bahadır, M.K. Sezgintürk, Applications of electrochemical immunosensors for early clinical diagnostics, Talanta 132 (2015) 162–174.
[36] B. Fatima, D. Hussain, S. Bashir, H.T. Hussain, R. Aslam, R. Nawaz, H.N. Rashid, N. Bashir, S. Majeed, M.N. Ashiq, Catalase immobilized antimonene quantum dots used as an electrochemical biosensor for quantitative determination of H2O2 from CA-125 diagnosed ovarian cancer samples, Mater. Sci. Eng. C 117 (2020), 111296.
[37] M.M. Rahman, T.A. Sheikh, A.M. Asiri, M.R. Awual, Development of 3-methoxyaniline sensor probe based on thin Ag2O@La2O3 nanosheets for environmental safety, New J. Chem. 43 (2019) 4620–4632.
[38] M. Díaz-González, X. Muñoz-Berbel, C. Jiménez-Jorquera, A. Baldi, C. Fernández-Sánchez, Diagnostics using multiplexed electrochemical readout devices, Electroanalysis 26 (2014) 1154–1170.
[39] J. Wu, Z. Fu, F. Yan, H. Ju, Biomedical and clinical applications of immunoassays and immunosensors for tumor markers, TrAC, Trends Anal. Chem. 26 (2007) 679–688.
[40] H. Kivrak, K. Selcuk, O.F. Er, N. Aktas, Electrochemical cysteine sensor on novel ruthenium based ternary catalyst, Int. J. Electrochem. Sci. 16 (2021).
[41] K. Abbas, H. Znad, M.R. Awual, A ligand anchored conjugate adsorbent for effective mercury(II) detection and removal from aqueous media, Chem. Eng. J. 334 (2018) 432–443.
[42] J. Das, S.O. Kelley, Protein detection using arrayed microsensor chips: tuning sensor footprint to achieve ultrasensitive readout of CA-125 in serum and whole blood, Anal. Chem. 83 (2011) 1167–1172.
[43] M. Hasan, M.A. Shenashen, M.N. Hasan, H. Znad, M.S. Salman, R. Awual, Natural biodegradable polymeric bioadsorbents for efficient cationic dye encapsulation from wastewater, J. Mol. Liq. (2021) 323.
[44] H. Li, J. Qin, M. Li, C. Li, S. Xu, L. Qian, B. Yang, Gold-nanoparticle-decorated boron-doped graphene/BDD electrode for tumor marker sensor, Sensor. Actuator. B Chem. 302 (2020), 127209.
[45] M. Johari-Ahar, M. Rashidi, J. Barar, M. Aghaie, D. Mohammadnejad, A. Ramazani, P. Karami, G. Coukos, Y. Omidi, An ultra-sensitive impedimetric immunosensor for detection of the serum oncomarker CA-125 in ovarian cancer patients, Nanoscale 7 (2015) 3768–3779.
[46] M. Jafari, M. Hasanzadeh, E. Solhi, S. Hassanpour, N. Shadjou, A. Mokhtarzadeh, A. Jouyban, S. Mahboob, Ultrasensitive bioassay of epitope of Mucin-16 protein (CA 125) in human plasma samples using a novel immunoassay based on silver conductive nano-ink: a new platform in early stage diagnosis of ovarian cancer and efficient management, Int. J. Biol. Macromol. 126 (2019) 1255–1265.
[47] L. Wu, Y. Sha, W. Li, S. Wang, Z. Guo, J. Zhou, X. Su, X. Jiang, One-step preparation of disposable multi-functionalized g-C3N4 based electrochemiluminescence immunosensor for the detection of CA125, Sensor. Actuator. B Chem. 226 (2016) 62–68.
[48] M. Hasanzadeh, R. Sahmani, E. Solhi, A. Mokhtarzadeh, N. Shadjou, S. Mahboob, Ultrasensitive immunoassay of carcinoma antigen 125 in untreated human plasma samples using gold nanoparticles with flower like morphology: a new platform in early stage diagnosis of ovarian cancer and efficient management, Int. J. Biol. Macromol. 119 (2018) 913–925.
[49] A. Ravalli, G.P. Dos Santos, M. Ferroni, G. Faglia, H. Yamanaka, G. Marrazza, New label free CA125 detection based on gold nanostructured screen-printed electrode, Sensor. Actuator. B Chem. 179 (2013) 194–200.
[50] S. Chen, R. Yuan, Y. Chai, L. Min, W. Li, Y. Xu, Electrochemical sensing platform based on tris (2, 2′-bipyridyl) cobalt (III) and multiwall carbon nanotubes–Nafion composite for immunoassay of carcinoma antigen-125, Electrochim. Acta 54 (2009) 7242–7247.
[51] D. Tang, B. Su, J. Tang, J. Ren, G. Chen, Nanoparticle-based sandwich electrochemical immunoassay for carbohydrate antigen 125 with signal enhancement using enzyme-coated nanometer-sized enzyme-doped silica beads, Anal. Chem. 82 (2010) 1527–1534.
[52] S.R. Torati, K.C. Kasturi, B. Lim, C. Kim, Hierarchical gold nanostructures modified electrode for electrochemical detection of cancer antigen CA125, Sensor. Actuator. B Chem. 243 (2017) 64–71.
[53] X.H. Fu, Electrochemical immunoassay for carbohydrate antigen-125 based on polythionine and gold hollow microspheres modified glassy carbon electrodes, Electroanalysis: Int. J. Devoted Fund. Pract.Aspects of Electroanalysis 19 (2007) 1831–1839.
[54] L. Wu, J. Chen, D. Du, H. Ju, Electrochemical immunoassay for CA125 based on cellulose acetate stabilized antigen/colloidal gold nanoparticles membrane, Electrochim. Acta 51 (2006) 1208–1214.
[55] K.B. Paul, V. Singh, S.R.K. Vanjari, S.G. Singh, One step biofunctionalized electrospun multiwalled carbon nanotubes embedded zinc oxide nanowire interface for highly sensitive detection of carcinoma antigen-125, Biosens. Bioelectron. 88 (2017) 144–152.
[56] Y. Zheng, H. Wang, Z. Ma, A nanocomposite containing Prussian Blue, platinum nanoparticles and polyaniline for multi-amplification of the signal of voltammetric immunosensors: highly sensitive detection of carcinoma antigen 125, Microchim. Acta 184 (2017) 4269–4277.
[57] Q. Zhu, Y. Chai, R. Yuan, Y. Zhuo, Simultaneous detection of four biomarkers with one sensing surface based on redox probe tagging strategy, Anal. Chim. Acta 800 (2013) 22–28.
[58] D. Tang, R. Yuan, Y. Chai, Electrochemical immuno-bioanalysis for carcinoma antigen 125 based on thionine and gold nanoparticles-modified carbon paste interface, Anal. Chim. Acta 564 (2006) 158–165.
[59] L. Wu, F. Yan, H. Ju, An amperometric immunosensor for separation-free immunoassay of CA125 based on its covalent immobilization coupled with thionine on carbon nanofiber, J. Immunol. Methods 322 (2007) 12–19.
[60] J. Wang, S.-T. Yau, Field-effect amperometric immuno-detection of protein biomarker, Biosens. Bioelectron. 29 (2011) 210–214.
[61] O.F. Er, B. Ulas, O. Ozok, A. Kivrak, H. Kivrak, Design of 2-(4-(2-pentyllbenzo b thiophen-3-yl)benzylidene)malononitrile based remarkable organic catalyst towards hydrazine electrooxidation, J. Electroanal. Chem. (2021) 888.
[62] F. Ciucci, Modeling electrochemical impedance spectroscopy, Curr. Opin. Electrochem. 13 (2019) 132–139.
[63] M.R. Awual, Solid phase sensitive palladium(II) ions detection and recovery using ligand based efficient conjugate nanomaterials, Chem. Eng. J. 300 (2016) 264–272.